Assessment of a Hybrid (Wind-Solar) System at High-Altitude Agriculture Regions for achieving Sustainable Development Goals

Youssef Kassem
Department of Mechanical Engineering, Engineering Faculty, Near East University, Nicosia, Cyprus | Energy, Environment, and Water Research Center, Near East University, Nicosia, Cyprus | Research Center for Science, Technology and Engineering (BILTEM), Near East University, Nicosia, Cyprus
yousseuf.kassem@neu.edu.tr (corresponding author)

Huseyin Camur
Department of Mechanical Engineering, Engineering Faculty, Near East University, Nicosia, Cyprus | Research Center for Science, Technology and Engineering (BILTEM), Near East University, Nicosia, Cyprus
huseyin.camur@neu.edu.tr

Ehsan Golzar Ghoshouni
Department of Mechanical Engineering, Engineering Faculty, Near East University, Nicosia, Cyprus
ehsanemu@yahoo.com.

Received: 10 October 2023 | Revised: 3 November 2023 | Accepted: 19 November 2023

 DOI: https://doi.org/10.48084/etasr.6494

ABSTRACT

Power generation from hybrid renewable energy systems is gaining popularity worldwide, especially in developing countries suffering from electricity crises. Small-scale hybrid wind and solar systems, especially in high-altitude agriculture regions, which may experience electricity shortages during extreme weather conditions, can be critical to achieving sustainability goals and objectives. The latter will be reached by providing clean energy and addressing economic concerns. Accordingly, the main aim of the current paper is to evaluate the techno-economic feasibility of a grid-connected hybrid (vertical axis wind turbine – 2-axis photovoltaic) system at high-altitude agriculture regions (Ardal and Faridan) in Iran for the production of clean energy. To this aim, the wind speed and solar radiation data were analyzed statistically using 13 distribution functions. The results indicate that Generalized Extreme Value produced the best fit for the wind speed and solar radiation data. Furthermore, the purpose of the current work is to evaluate the technical and economic aspects of grid-connected hybrid vertical axis wind turbines as well as PV tracking systems using RETScreen software. The results demonstrate that implementing the proposed system could generate significant amounts of electricity in order to meet the demand for domestic and agricultural applications while ensuring clean energy in line with sustainable development goals. Besides, this study can help integrate renewable energy into the grid and help policymakers facilitate the installation of rooftop small-scale hybrid systems in the future.

Keywords-wind; solar; techno-economic; hybrid system; vertical axis wind turbine; PV tracking systems

I. INTRODUCTION

The Sustainable Development Goals include seventeen global goals set by the United Nations General Assembly to promote a sustainable future for all [1]. These goals were officially adopted in 2015, with the aim to accomplish their widespread implementation by 2030 [2]. Concerning the Sustainable Development Goals, the advancement of renewable energy sources plays a pivotal role in achieving energy security in various sectors, including transportation, environmental conservation, construction, economy, machinery, and industry [3]. Energy derived from renewable energy sources such as solar and wind energy, effectively meets the energy requirements while simultaneously promoting community development and global environmental conservation [4]. Renewable energy has emerged as a powerful solution to the energy crisis during the recent decades, offering a way to address the challenge while mitigating adverse impacts on climate and nature [5-7].

At present, Iran's heavy dependence on fossil fuels, especially natural gas and oil, has led to the need to diversify energy sources [8]. According to the World Bank, fossil fuel energy consumption accounts for approximately 99.02% of the total energy consumption, with the remaining 0.08% sourced from renewable energy. Therefore, energy remains a significant challenge in the country, despite the government's ongoing efforts to respond to the energy necessities of the population. The, electric power consumption in Iran generally ranges from 2.31 to 5.67 kWh per capita (i.e. 2.927 kWh per capita) according to the World Bank. Consequently, there is a pressing need to fully harness the proven vast reserves of renewable energy resources to complement traditional energy sources, mitigate impending energy crises, and enhance electricity access for sustainable national development. Wind and solar energy are vital tools in the fight against climate change as the world confronts the escalating threat of global warming [9-11]. Their adoption is a strategic step toward a sustainable future [11]. Wind turbines and photovoltaic (PV) panels generate clean electricity, minimizing greenhouse gas emissions and reducing the carbon footprint [12]. Utilizing wind and solar energy can significantly reduce the reliance on fossil fuels, transforming the energy landscape [13]. This diversification enhances Iran's energy security, reducing the vulnerability to supply disruptions and price fluctuations in the global energy market.

The main goal of this paper is to evaluate the feasibility of harnessing wind energy and analyze the effectiveness of a grid-connected vertical axis wind turbine combined with a tracking photovoltaic system in high-altitude regions. In regions characterized by high altitudes, access to traditional energy grids can be limited, emphasizing the importance of renewable energy systems like wind and solar for meeting local energy demands [14]. Furthermore, the implementation of grid-connected renewable energy systems can enhance energy self-sufficiency and reduce reliance on long-distance energy transmission [15]. Accordingly, it is essential to assess the wind energy potential and the performance of grid-connected vertical axis wind turbines with tracking PV systems in high-altitude areas. These regions often feature stronger and more consistent wind resources, which can contribute to the expansion of renewable energy, decrease environmental impact, and bolster energy security in remote locations.

II. MATERIALS AND METHODS

A. Study Area

Ardal (Latitude: 31.99°N, Longitude: 50.66°E, elevation: 1847 m) and Faridan (Latitude: 32.98°N, Longitude: 50.39°E, elevation: 2267 m) are two high-altitude areas located in Iran. Ardal and Faridan are regions located in the Chaharmahal and Bakhtiari Province in southwestern Iran and the Isfahan Province of central Iran, respectively. The economy of these selected locations is primarily based on agriculture, animal husbandry, and pastoral activities. In general, due to climate variability, agricultural demand, and changes in land use, both locations face the challenges of water scarcity. Moreover, both locations can experience extreme weather conditions, such as heavy snowfall, which can damage power lines and disrupt electricity supply.

B. Data Collection

The Modern-Era Retrospective Analysis for Research and Applications, Version 2 (MERRA-2), is a reanalysis dataset provided by NASA that offers a comprehensive record of the Earth's climate from 1980 onward [16]. MERRA-2 is an updated version of the original MERRA dataset, providing more accurate and detailed atmospheric data and climate information. It is commonly used by researchers and scientists for various climate, weather, and environmental studies [5, 13, 17-20]. MERRA-2 covers a wide range of atmospheric and environmental variables, including temperature, humidity, wind, precipitation, radiation, and more [21]. These variables are available at multiple altitudes and spatial resolutions. Additionally, it offers data on a global scale, making it suitable for research and analysis in various regions around the world. The mean monthly wind speed including minimum and maximum wind speed and solar radiation data were collected from 1981 to 2022 and 2001-2022, respectively.

C. Grid-on Wind-PV Hybrid System

A grid-connected Vertical Axis Wind Turbine (VAWT) and tracking photovoltaic (PV) system represent two distinct renewable energy technologies that can be integrated to generate electricity efficiently and sustainably. Combining a VAWT system with a tracking PV system allows for the simultaneous capture of wind and solar energy. This combination of renewable energy sources can contribute to a more reliable and sustainable energy supply, especially in areas with variable weather conditions [22]. In general, the grid-connected VAWT and PV components are summarized in Table I.

TABLE I. COMPONENTS OF A WIND AND PV SYSTEM [13]

Grid-connected VAWT	Tracking PV system
VAWT: The central component of the system is the VAWT itself, which consists of vertical rotor blades connected to a vertical shaft. The rotor blades capture wind energy and transfer it to the generator.	Solar panels: Also known as PV modules, are made up of multiple solar cells that convert sunlight into electricity. In a tracking PV system, these panels are mounted on tracking structures.
Generator: The generator is responsible for converting the mechanical energy from the rotating VAWT blades into AC electrical energy.	Tracking Mechanism: The tracking mechanism includes motors and sensors that allow the solar panels to follow the sun's path across the sky. It can be a single-axis tracker, which follows the sun's east-west movement, or a dual-axis tracker, which follows both east-west and north-south movements.
Inverter: It is used to convert the AC generated by the VAWT into DC. This DC electricity can then be conditioned and synchronized with the grid's electrical characteristics.	Inverter: Converts the DC electricity generated by the solar panels into AC electricity compatible with the grid.
Grid Connection: A connection point to the electrical grid allows the system to feed the generated electricity into the grid for distribution and use.	Grid Connection: The PV system is connected to the electrical grid through a grid connection point, enabling the electricity generated by the solar panels to be fed into the grid.

The electricity generated by the VAWT and the PV systems is synchronized through inverters to ensure it is compatible with the grid's electrical characteristics [23]. The combined output of wind and solar energy is then fed into the electrical grid for distribution and use. Calculating the capacity of an inverter for integrating a VAWT and a tracking PV system requires consideration of various factors, including the maximum power output of each system, their respective voltage levels, and any potential surges in power production. It can be done as follows:

- Determine the Maximum Power Outputs: Find out the maximum power output of the VAWT and the tracking PV system. These ratings represent the peak power that each system can produce under optimal conditions.
- Voltage Compatibility: (1) Determine the voltage output of the VAWT system. The VAWT often generates low-voltage DC power. (2) Determine the voltage output of your tracking PV system. Solar panels typically produce low-voltage DC power. Ensure that both systems' voltage levels are compatible with the chosen inverter. In most grid-connected systems, an inverter converts DC to AC power for grid synchronization.
- Add the peak power output of your VAWT system to the peak power output of your tracking PV system to get the total peak power.

It is common to oversize the inverter slightly to accommodate power surges or fluctuations. A 10-20% safety margin is often recommended. Selecting the right inverter capacity is crucial for the efficient and safe integration of your VAWT and tracking PV systems into the grid. Oversizing the inverter slightly and considering safety margins can help ensure that your renewable energy system performs optimally under varying conditions.

D. Probability Density Functions (PDFs)

PDFs provide a systematic way to analyze and understand the statistical properties of wind speed and solar radiation data [13]. They help summarize the data, making it easier to grasp central tendencies, variability, and extremes within the dataset. PDFs allow modeling the behavior of wind speed and solar radiation, which is crucial in various applications. PDFs are used to estimate the long-term energy potential of a location in renewable energy resource assessment [24]. This information is crucial for project development and investment decisions. In this study, 13 distribution functions (DFs) are utilized to represent the wind speed and solar radiation frequency distribution. These distributions are listed in Table II.

E. Wind Potential Estimation

Wind Power Density (WPD) is one of the most important indicators of wind potential for designing a wind farm. WPD is an indicator used to assess the potential of wind resources at a particular location. It can be determined by [25]:

$$\frac{\bar{P}}{A} = \frac{1}{2}\rho\bar{v}^3 \qquad (1)$$

where P represents the wind power, ρ is the air density ($\rho = 1.23\ \mathrm{kg/m^3}$), and $\bar{v}$ is the mean wind speed in m/s.

Furthermore, the wind energy potential is categorized according to the average WPD at 10 m height [13, 25].

- Poor (WPD ≤100 W/m^2)
- Marginal (WPD ≤150 W/m^2)
- Moderate (WPD ≤200 W/m^2)
- Good (WPD ≤250 W/m^2)
- Excellent (WPD ≤300 W/m^2)

Wind speed data are typically collected at a consistent height of 10 m above the ground. To estimate wind speeds at different hub heights, the power law model is employed. This model is defined by [25]:

$$\frac{v}{v_{10}} = \left(\frac{z}{z_{10}}\right)^{\alpha} \qquad (2)$$

where v is the wind speed at the wind turbine hub height z, v_{10} is the wind speed at the original height z_{10}, and α is the surface roughness coefficient, which depends on the characteristics of the region. The value of α can be determined by [25]:

$$\alpha = \frac{0.37-0.088\ln(v_{10})}{1-0.088\ln(z_{10}/2)} \qquad (3)$$

F. Solar Potential Estimation

Solar energy potential was evaluated by categorizing it based on the annual Global Solar Radiation (GSR) amounts. GSR is considered a key parameter for assessing the energy generation potential of PV systems. The solar energy potential is classified based on the annual value of GSR as described below [10]:

- Poor (Annual GSR <1191.8 kWh/m^2)
- Marginal (1191.8<Annual GSR <1419.7kWh/m^2)
- Fair (1419.7<Annual GSR <1641.8 kWh/m^2)
- Good (1641.8<Annual GSR <1843.8 kWh/m^2)
- Excellent (1843.8<Annual GSR <2035.9 kWh/m^2)
- Outstanding (2035.9<Annual GSR <2221.8kWh/m^2)
- Superb (Annual GSR <2221.8kWh/m^2)

G. The Proposed Hybrid System

In this study, the viability of developing a 5 kW grid-connected hybrid system was examined from technical, financial, and environmental perspectives. Additionally, the monocrystalline silicon (mono-Si) PV module with the model JKM360M-76, featuring a power capacity of 360 W and an efficiency of 18.55%, was employed. The detailed specifications of the chosen PV module can be found in Table III. Furthermore, the SunSurfs WT3 Vertical Axis Wind Turbine with a rated capacity of 5 kW was chosen. The detailed specifications of the selected turbine are provided in Table IV.

TABLE II. DFS, PDFS, AND CUMULATIVE DFS

Distribution Function	Probability Density Function	Cumulative Distribution Function
Normal (N)	$f(v) = \frac{1}{\sqrt{2\pi\sigma^2}} exp\left(-\frac{v-\mu}{2\sigma^2}\right)$	$F(v) = \frac{1}{2}\left[1 + erf\left(\frac{v-\mu}{\sigma\sqrt{2}}\right)\right]$
Gamma (G)	$f(v) = \frac{R^{\alpha-1}}{\beta^{\alpha}\Gamma(\alpha)} exp\left(-\left(\frac{v}{\beta}\right)\right)$	$F(v) = \frac{\Gamma_{R/\beta}(\alpha)}{\Gamma(\alpha)}$
Generalized Extreme Value (GEV)	$f(v) = \begin{cases} \frac{1}{\sigma}\left[\left(1+\zeta\left(\frac{v-\mu}{\sigma}\right)\right)^{-1/\zeta}\right]^{\zeta+1} exp\left(-\left(1+\zeta\left(\frac{v-\mu}{\sigma}\right)\right)^{-1/\zeta}\right) & k \neq 0 \\ \frac{1}{\sigma}\left[exp\left(-\left(\frac{v-\mu}{\sigma}\right)\right)\right]^{\zeta+1} exp\left(exp\left(-\left(\frac{v-\mu}{\sigma}\right)\right)\right) & k = 0 \end{cases}$	$F(v) = \begin{cases} exp\left(-exp\left(-\left(\frac{v-\mu}{\sigma}\right)\right)\right) & k \neq 0 \\ exp\left(-exp\left(-\frac{v-\mu}{\sigma}\right)\right) & k = 0 \end{cases}$
Nakagami (Na)	$f(v) = \frac{2m^m}{\Gamma(m)\Omega^{\mathrm{m}}} v^{2m-1} e^{\left(-\frac{m}{\Omega}G^2\right)}$	$F(v) = \frac{\gamma\left(m,\frac{m}{\Omega}v^2\right)}{\Gamma(m)}$
Inverse Gaussian (IG)	$f(v) = \sqrt{\frac{\lambda}{2\pi(R-\gamma)}} exp\left(-\frac{\lambda(v-\mu)^2}{2\mu^2 R}\right)$	$F(v) = \Phi\left(\sqrt{\frac{\lambda}{R-\gamma}}\left(\frac{v}{\mu}-1\right)\right) + \Phi\left(-\sqrt{\frac{\lambda}{R-\gamma}}\left(\frac{v}{\mu}+1\right)\right) exp\left(\frac{2\lambda}{\mu}\right)$
Log-normal (LN)	$f(v) = \frac{1}{v\sigma\sqrt{2\pi}} exp\left[-\frac{1}{2}\left(\frac{ln(v)-\mu}{\sigma}\right)^2\right]$	$F(v) = \frac{1}{2} + erf\left[\frac{ln(v)-\mu}{\sigma\sqrt{2}}\right]$
Log-Logistic (LL)	$f(v) = \left(\left(\frac{\beta}{\alpha}\left(\frac{v}{\alpha}\right)^{\beta-1}\right) \Big/ \left(1+\frac{v}{\alpha}\right)^{\beta}\right)^2$	$F(v) = \frac{1}{\left(1+\frac{v}{\alpha}\right)^{-\beta}}$
Rayleigh (R)	$f(v) = \frac{v}{\sigma^2} exp\left(-\frac{1}{2}\left(\frac{v}{\sigma}\right)^2\right)$	$F(v) = 1 - exp\left(-\frac{1}{2}\left(\frac{v}{\sigma}\right)^2\right)$
Weibull (W)	$f(v) = \left(\frac{\alpha}{\sigma}\right)\left(\frac{v}{\sigma}\right)^{\alpha-1} exp\left(-\left(\frac{v}{\sigma}\right)^{\alpha}\right)$	$F(v) = 1 - exp\left(-\left(\frac{v}{\sigma}\right)^{\alpha}\right)$
Three-Parameter Weibull (W-3P)	$f(v) = \left(\frac{\alpha}{\beta}\right)\left(\frac{v-\gamma}{\beta}\right)^{\alpha-1} exp\left(-\left(\frac{v-\gamma}{\beta}\right)^{\alpha}\right)$	$F(v) = 1 - exp\left(-\left(\frac{v-\gamma}{\beta}\right)^{\alpha}\right)$
Kumaraswamy (K)	$f(v) = \frac{abe^{\left(-\frac{1-(1-v^a)^b}{\beta(1-v^a)^b}\right)}}{\Gamma(\alpha)\beta^{\alpha}} \frac{1}{(1-v^a)^2}\left(\frac{1-(1-v^a)^b}{\beta(1-v^a)^b}\right)^{\alpha-1}$	$F(v) = \int_0^{\frac{1-(1-v^a)^b}{(1-v^a)^b}} \frac{e^{\frac{-\omega}{\beta}}}{\Gamma(\alpha)\beta^{\alpha}} d\omega = \frac{\Gamma(\alpha,z)}{\Gamma(\alpha)\beta^{\alpha}}\left(\alpha, \frac{1-(1-v^a)^b}{\beta(1-v^a)^b}\right)$
Birnbaum-Saunders (BS)	$f(v) = \frac{\sqrt{\frac{v-\mu}{\beta}}+\sqrt{\frac{\beta}{v-\mu}}}{2\gamma(v-\mu)} \phi\left(\frac{\sqrt{\frac{v-\mu}{\beta}}-\sqrt{\frac{\beta}{v-\mu}}}{\gamma}\right)$	$F(v) = \Phi\left(\frac{\sqrt{v}-\sqrt{\frac{1}{v}}}{\gamma}\right)$
Logistic (L)	$f(v) = \frac{exp\left(-\frac{v-\mu}{\sigma}\right)}{\sigma\left\{1+exp\left(-\frac{v-\mu}{\sigma}\right)\right\}^2}$	$F(v) = \frac{1}{1+exp(-v)}$

N	σ	Standard deviation	Na	m	Shape parameter	LL	β	Shape parameter
	μ	Mean parameter		Ω	Scale parameter		α	Scale parameter
G	β	Shape parameter	IG	λ	Shape parameter	W	α	Shape parameter
	α	Scale parameter		μ	Mean parameter		σ	Scale parameter
GEV	μ	Location parameter	LN	σ	Shape parameter	W-3P	α	Shape parameter
	α	Scale parameter		μ	Scale parameter		σ	Scale parameter
	ζ	Shape parameter	R	σ	Scale parameter		γ	Location parameter
K	a	Shape parameter	BS	μ	Location parameter	L	μ	Location parameter
	b	Shape parameter		β	Scale parameter		σ	Scale parameter
	α	Shape parameter		γ	Shape parameter			
	β	Scale parameter						

TABLE III. SPECIFICATION OF THE SELECTED PV PANEL

Item	Specification	
Manufacturer	JinKO solar	
Model	JKM545M-72HL4-V	
	STC	NOCT
Maximum power (P_{max}) [W]	545	405
Voltage at maximum power (*Vmp*) [V]	40.8	38.25
Current at maximum power (*Impp*) [A]	13.36	10.60
Open circuit voltage (*Voc*) [V]	49.52	46.74
Short circuit current (*Isc*) [A]	13.94	11.26
Operating temperature range [℃]	-40℃~+85℃	
Temperature coefficient of P_{max} [%/℃]	-0.35%/℃	
Temperature coefficient of Voc [%/℃]	-0.28%/℃	
Temperature coefficient of Isc [%/℃]	0.048%/℃	
Nominal operating cell temperature (NOCT)	45±2℃	
Cost [USD/W]	0.37	

TABLE IV. WIND TURBINE CHARACTERISTICS

Variable	Value
Rated power [kW]	5
Startup wind speed [m/s]	1.8
Rated wind speed [m/s]	10
Survival wind speed [m/s]	28
Rated rotating speed [rpm]	40
Diameter [m]	18
Tower height [m]	14
Cost [USD]	15300

H. Simulation Software

Recently, various simulation tools have been utilized for evaluating the performance of wind farms, solar plants, and hybrid systems [20]. RETScreen is a widely used software tool for assessing energy production, life-cycle costs, emission reduction, financial viability, and risk for various types of renewable energy and energy efficiency projects [7]. It can be employed to rate the feasibility of grid-connected VAWTs and PV tracking systems, among other renewable energy projects. RETScreen is a versatile software tool that can appraise the technical and financial aspects of such hybrid renewable energy projects [7, 6].

Equations (4)-(11) represent the pre-defined mathematical expressions used by the tool [6, 7, 24] to perform the economic evaluation.

Capacity Factor (CF):

$$\mathrm{CF} = \frac{P_{out}}{P \times 8760} \tag{4}$$

Annual GHG emission reduction (A-GHG):

$$\mathrm{A-GHG} = [(Base\ case\ GHG\ emission\ factor) - (Proposed\ \ case\ GHG\ emission\ factor)] \times End\ use\ energy\ delivered \tag{5}$$

Net Present Value (NPV):

$$\mathrm{NPV} = \sum_{n=0}^{N} \frac{C_n}{(1+r)^n} \tag{6}$$

Levelized cost of energy (LCOE):

$$\mathrm{LCOE} = \frac{sum\ of\ cost\ over\ lifetime}{s\ of\ electricity\ generated\ over\ lifetime} \tag{7}$$

Simple Payback (SP):

$$\mathrm{SP} = \frac{C - IG}{(C_{ener} + C_{capa} + C_{RE} + C_{GHG}) - (C_{o\&M} + C_{fuel})} \tag{8}$$

Equity Payback (EP):

$$\mathrm{EP} = \sum_{n=0}^{N} C_n \tag{9}$$

Annual Life Cycle Savings (ALCS):

$$\mathrm{ALCS} = \frac{NPV}{\frac{1}{r}\left(1 - \frac{1}{(1+r)^N}\right)} \tag{10}$$

Benefit-Cost (B-C) ratio:

$$\mathrm{B-C} = \frac{NPV + (1-f_d)C}{(1-f_d)C} \tag{11}$$

where P_{out} is the energy generated per year, P is the installed capacity, N is the project life in years, C_n is the after-tax cash flow in year n, r is the discount rate, C is the total initial cost of the project, f_d is the debt ratio, B is the total benefit of the project, IG represents the incentives and grants, C_{ener} is the annual energy savings or income. C_{capa} is the annual capacity savings or income, C_{RE} is the annual Renewable Energy (RE) production credit income, C_{GHG} is the GHG reduction income, $C_{o\&M}$ is the yearly operation and maintenance costs incurred by the clean energy project, C_{fuel} is the annual cost of fuel, which is zero for renewable projects, and Δ_{GHG} is the annual GHG emission reduction.

III. RESULTS AND DISCUSSION

A. Assessment of Wind Energy Potential

Figure 1 shows the mean monthly variation of wind speed for the selected locations. The statistical description of average monthly wind speed includes mean, Standard Deviation (SD), Coefficient of Variation (CV), minimum (Min.), maximum (Max.), Kurtosis (K), and Skewness (S), which are summarized in Table V. It is found that the mean wind speeds are within the range of 2.51-3.07 m/s for Ardal and 3.14-3.89 m/s for Faridan. Generally, the mean and SD values indicate a high level of consistency in wind behavior. Furthermore, it is evident that the CV values exhibit moderate levels, spanning from 10.21% to 24.5% for Ardal and 10.58% to 28.35% for Faridan. Additionally, we observe that the lowest monthly wind speeds, 1.81 m/s and 2.12 m/s, were recorded in November 2010 and November 1996, respectively. On the other hand, Faridan records the highest monthly wind speed at 6.48 m/s. Moreover, most locations display positive S values, signaling right-skewed data distributions. The K values, ranging from -1.56 to 7.79, signify variations in the flatness of the data distributions. A negative kurtosis (-1.56) suggests a slightly flatter distribution, while a positive kurtosis (7.79) implies heavier-tailed data compared to a normal distribution. As mentioned above, 13 distribution functions were utilized for analyzing the characteristics of wind speed at the selected location. Based on the findings, the GEV distribution function offers superior fits (best Kolmogorov-Smirnov (KS) values) for the wind speed data as shown in Table VI. Figure 2 involves the graphical representation of the PDF for all selected DFs. To assess the wind potential at the chosen location, the WPD was calculated. Its values were 13.97 W/m^2 and 26.48 W/m^2 for Ardal and

Faridan, respectively. Based on the WPD values obtained, the selected locations fall into power class 1, signifying relatively poor wind energy potential. Therefore, it is most suitable to utilize small-scale wind turbines in these regions to harness the available wind energy resources effectively.

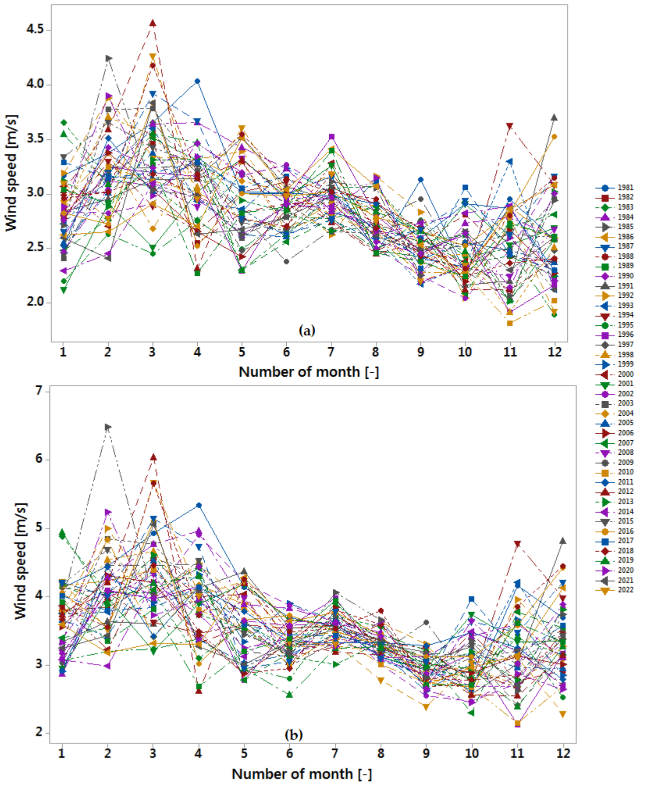

Fig. 1. Monthly variation of mean wind speed for (a) Ardal, (b) Faridan.

B. Assessment of Solar Energy Potential

Figure 3 illustrates the mean monthly variation of Solar Radiation (SR) for the chosen locations. The statistical description of monthly average SR is summarized in Table VII. The mean monthly SR falls within the range of 5.54-6.29 kWh/m^2/day for Ardal and 5.16-6.14 kWh/m^2/day for Faridan, suggesting a notably consistent pattern based on the mean and standard deviation values. Furthermore, the S values for most locations are positive, denoting that all the distributions are right-skewed. It is found that the annual value of GHI is 2280.89 kWh/m^2 for Ardal and 2235.06 kWh/m^2 for Faridan. The analysis reveals that the solar resources in the chosen locations are categorized into the superb potential. In addition, the chosen DFs parameters were determined using the maximum likelihood method with monthly SR data. To ascertain the most appropriate distribution among the ten options for each location, the Kolmogorov-Smirnov (KS) test was employed. Table VIII provides a summary of the estimated distribution parameters for all selected models, including the KS values and their corresponding ranks. According to the results, the GEV distribution function demonstrated the lowest KS value, implying that it offers the best fit for the SR data.

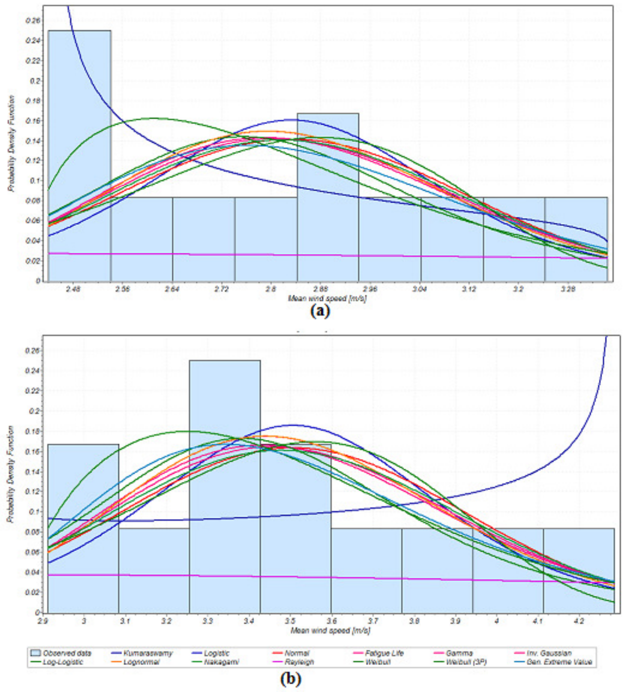

Fig. 2. Comparisons of PDF distributions for analyzing wind speed data (a) Ardal, (b) Faridan.

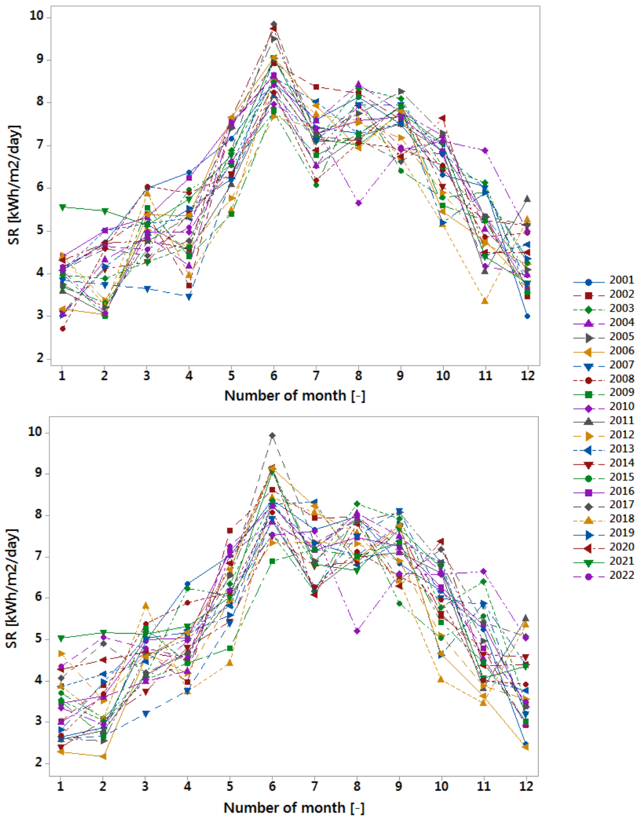

Fig. 3. Monthly variation of mean SR for (a) Ardal, (b) Faridan.

Figure 4 illustrates the graphical representation of the PDFs for all selected DFs.

C. Techno-Economic Analysis

Techno-Economic Analysis (TEA) for a grid-connected hybrid renewable energy system is crucial for financial decision-making. TEA helps assess the economic feasibility of the project by estimating costs, revenues, and potential returns on investment. This information is vital for investors, project developers, and financial institutions to make informed decisions. Also, it helps quantify reductions in greenhouse gas emissions and other pollutants, contributing to sustainability goals. In this study, TEA for the developed system was conducted using the RETScreen software. To make the system feasible, this study utilizes various financial parameters as input variables, such as 7% inflation rate, 12% discount rate, 9% reinvestment rate, 70% debt ratio, 0% debt interest rate, and 5% electricity export escalation rate. These values were assumed based on previous scientific studies.

Figure 5 depicts the monthly Electricity Generation Exported (EGE) to the grid by a 5 kW grid-connected hybrid system. The data shows that the highest EGE values occur in June for the PV system and in March for the wind system. Conversely, the lowest EGE values are observed in December for the PV system and in September for the wind system.

TABLE V. STATISTICAL DESCRIPTION OF AVERAGE MONTHLY WIND SPEED FOR ALL SELECTED LOCATIONS

Year	Ardal							Faridan						
	Mean	SD	CV	Min.	Max.	S	K	Mean	SD	CV	Min.	Max.	S	K
1981	3.07	0.49	16.09	2.28	4.04	0.30	0.26	3.89	0.80	20.51	2.63	5.34	0.18	-0.36
1982	2.80	0.31	10.98	2.37	3.46	0.68	0.70	3.39	0.44	12.97	2.76	4.20	0.21	-0.61
1983	2.87	0.41	14.22	2.25	3.66	0.11	-0.26	3.54	0.58	16.40	2.81	4.88	1.06	1.31
1984	2.95	0.45	15.29	2.27	3.66	0.36	-0.93	3.71	0.70	18.75	2.69	4.96	0.47	-0.29
1985	2.87	0.54	18.85	2.06	4.25	1.28	3.72	3.77	0.98	25.84	2.61	6.48	2.01	5.80
1986	2.89	0.36	12.42	2.28	3.51	0.21	-0.33	3.45	0.46	13.24	2.70	4.27	0.35	-0.21
1987	2.96	0.44	14.90	2.57	3.92	1.34	0.86	3.77	0.71	18.78	2.94	5.14	0.58	-0.50
1988	3.06	0.48	15.83	2.31	4.18	0.82	2.06	3.79	0.79	20.72	2.68	5.66	0.94	2.34
1989	2.75	0.38	13.68	2.24	3.40	0.24	-0.85	3.32	0.45	13.60	2.68	3.94	-0.17	-1.06
1990	2.90	0.40	13.96	2.14	3.46	-0.29	-0.56	3.59	0.49	13.59	2.65	4.43	-0.30	0.17
1991	2.90	0.47	16.18	2.16	3.70	-0.06	-0.35	3.59	0.61	16.92	2.57	4.81	0.54	0.49
1992	3.00	0.48	16.03	2.04	3.88	-0.22	0.54	3.71	0.64	17.15	2.55	4.99	0.32	0.75
1993	2.79	0.46	16.30	2.12	3.60	0.13	-0.63	3.53	0.50	14.15	2.84	4.34	0.13	-1.17
1994	2.88	0.38	13.23	2.20	3.63	0.22	0.44	3.64	0.50	13.59	2.75	4.78	0.70	2.24
1995	2.51	0.27	10.56	1.89	2.79	-1.18	1.59	3.14	0.33	10.58	2.52	3.65	-0.39	-0.49
1996	2.75	0.49	17.88	1.91	3.53	-0.11	-0.86	3.33	0.63	18.80	2.12	4.15	-0.25	-0.52
1997	2.75	0.44	15.86	2.03	3.66	0.52	0.65	3.49	0.63	17.97	2.41	4.57	0.32	-0.51
1998	2.84	0.51	17.91	1.91	3.71	0.08	-0.11	3.52	0.62	17.62	2.70	4.66	0.74	-0.30
1999	2.80	0.37	13.30	2.24	3.28	-0.23	-1.56	3.47	0.57	16.45	2.61	4.32	0.10	-1.22
2000	2.81	0.45	15.90	2.11	3.55	0.15	-1.11	3.46	0.58	16.82	2.66	4.53	0.31	-0.83
2001	2.76	0.36	13.17	2.12	3.33	-0.04	-0.71	3.50	0.41	11.71	2.95	4.18	0.17	-1.13
2002	2.83	0.43	15.31	2.04	3.47	-0.43	-0.63	3.57	0.76	21.30	2.47	4.90	-0.03	-0.84
2003	2.87	0.48	16.84	2.41	3.79	1.23	0.31	3.57	0.65	18.15	2.95	4.84	1.30	0.61
2004	2.83	0.35	12.51	2.23	3.38	-0.05	-0.60	3.52	0.59	16.68	2.68	4.83	0.78	1.14
2005	2.71	0.30	10.90	2.37	3.38	1.13	1.06	3.30	0.46	13.97	2.72	4.52	1.72	4.23
2006	2.74	0.34	12.45	2.19	3.38	0.06	-0.11	3.40	0.49	14.43	2.87	4.31	0.85	-0.39
2007	2.74	0.39	14.29	2.08	3.51	0.49	0.65	3.44	0.58	16.79	2.29	4.41	-0.33	0.34
2008	2.80	0.32	11.53	2.24	3.33	-0.30	-0.39	3.36	0.51	15.32	2.68	4.33	0.57	-0.30
2009	2.73	0.39	14.31	2.12	3.27	0.08	-1.11	3.48	0.66	18.87	2.70	4.47	0.62	-1.04
2010	2.64	0.45	17.17	1.81	3.25	-0.52	-0.75	3.32	0.72	21.73	2.15	4.39	0.10	-1.17
2011	2.91	0.33	11.38	2.30	3.51	-0.10	0.35	3.45	0.47	13.52	2.79	4.43	0.88	0.72
2012	2.87	0.70	24.56	2.12	4.57	1.34	2.07	3.47	0.98	28.35	2.55	6.03	1.74	3.63
2013	2.83	0.36	12.78	2.01	3.32	-0.77	1.31	3.51	0.55	15.64	2.77	4.61	0.62	-0.22
2014	2.70	0.28	10.21	2.20	3.10	-0.62	-0.51	3.33	0.41	12.36	2.69	4.20	0.67	0.42
2015	2.94	0.40	13.66	2.48	3.66	0.58	-1.14	3.63	0.60	16.42	2.80	4.69	0.59	-0.74
2016	2.94	0.39	13.40	2.52	3.84	1.39	1.67	3.68	0.61	16.50	3.01	5.11	1.33	1.78
2017	2.93	0.38	12.81	2.30	3.29	-0.94	-0.80	3.58	0.41	11.41	2.70	4.13	-0.70	0.45
2018	2.75	0.33	11.94	2.24	3.18	-0.14	-1.41	3.38	0.54	16.00	2.77	4.45	0.51	-0.55
2019	2.85	0.50	17.56	2.02	3.56	0.14	-0.89	3.42	0.76	22.36	2.39	4.94	0.69	-0.24
2020	2.83	0.50	17.50	2.19	3.90	0.67	0.64	3.36	0.75	22.41	2.44	5.23	1.31	2.70
2021	2.71	0.40	14.58	2.30	3.84	2.36	6.71	3.38	0.57	16.89	2.69	5.05	2.46	7.79
2022	2.90	0.63	21.61	1.92	4.27	0.64	1.08	3.49	0.94	26.95	2.28	5.67	1.02	1.48

TABLE VI. DF PARAMETERS AND P-VALUE BASED ON THE KS TEST FOR ANALYZING WIND SPEED DATA

DF	Ardal			DF	Faridan		
	Parameters	**Statistic**	**Rank**		**Parameters**	**Statistic**	**Rank**
GEV	k=-0.16507 σ=0.27731 μ=2.7116	0.11588	1	GEV	k=-0.07426 σ=0.37932 μ=3.3123	0.10576	1
Na	m=24.819 Ω=8.095	0.13259	2	W-3P	α=1.6117 β=0.72886 γ=2.8493	0.11904	2
W	α=11.199 β=2.9025	0.13349	3	G	α=70.049 β=0.05004	0.12537	3
G	α=99.74 β=0.0284	0.13431	4	Na	m=17.104 Ω=12.447	0.1269	4
N	σ=0.28359 μ=2.8322	0.13655	5	LN	σ=0.11298 μ=1.2478	0.12784	5
LL	α=15.845 β=2.7759	0.14002	6	BS	α=0.1131 β=3.4828	0.1279	6
W-3P	α=1.4275 β=0.45671 γ=2.4141	0.14521	7	LL	α=13.698 β=3.4177	0.13203	7
BS	α=0.09561 β=2.8193	0.14568	8	N	σ=0.41879 μ=3.5051	0.13851	8
LN	σ=0.09554 μ=1.0365	0.14575	9	W	α=9.6125 β=3.6	0.14096	9
IV	λ=282.48 μ=2.8322	0.14717	10	IG	λ=245.53 μ=3.5051	0.14141	10
L	σ=0.15635 μ=2.8322	0.15788	11	L	σ=0.23089 μ=3.5051	0.15542	11
K	α_1=0.61943 α_2=1.1245 a=2.4402 b=3.3493	0.20313	12	K	α_1=0.91493 α_2=0.70462 a=2.7775 b=4.2843	0.26401	12
R	σ=2.2598	0.44181	13	R	σ=2.7967	0.4186	13

TABLE VII. STATISTICAL DESCRIPTION OF AVERAGE MONTHLY SOLAR RADIATION FOR ALL SELECTED LOCATIONS

Year	Ardal							Faridan						
	Mean	**SD**	**CV**	**Min.**	**Max.**	**S**	**K**	**Mean**	**SD**	**CV**	**Min.**	**Max.**	**S**	**K**
2001	6.28	1.66	26.48	2.99	8.47	-0.67	-0.18	5.71	2.10	36.75	2.46	8.38	-0.53	-1.09
2002	6.15	1.95	31.65	3.45	8.92	0.01	-1.61	5.69	2.09	36.68	2.92	8.62	0.08	-1.72
2003	5.98	1.86	31.04	3.55	8.49	0.01	-1.70	5.70	1.96	34.40	3.01	8.36	0.03	-1.56
2004	6.05	1.98	32.73	3.06	8.63	-0.09	-1.79	5.55	1.99	35.88	2.96	8.05	-0.06	-1.96
2005	6.16	2.01	32.62	3.20	9.49	0.03	-1.23	5.70	2.19	38.36	2.55	9.12	-0.09	-1.16
2006	5.86	2.01	34.25	3.03	9.06	0.04	-1.23	5.30	2.43	45.89	2.17	9.14	0.11	-1.35
2007	5.72	1.92	33.46	3.46	8.20	-0.02	-1.92	5.20	2.06	39.69	2.59	8.11	0.07	-1.58
2008	5.86	1.43	24.40	2.71	8.25	-0.67	1.21	5.47	1.59	29.03	2.68	8.08	-0.27	-0.63
2009	5.54	1.64	29.64	2.99	7.92	0.07	-1.09	5.16	1.66	32.16	2.65	7.36	-0.02	-1.33
2010	5.88	1.49	25.38	3.07	7.96	-0.45	-0.72	5.56	1.56	28.00	2.95	7.62	-0.36	-0.99
2011	5.71	1.64	28.80	3.06	8.17	-0.20	-1.14	5.35	1.74	32.56	2.57	7.86	-0.33	-1.11
2012	5.64	1.49	26.36	3.36	7.67	0.17	-1.44	5.37	1.53	28.50	3.52	7.36	0.26	-1.70
2013	6.14	1.54	25.12	4.07	8.60	0.19	-1.52	5.74	1.73	30.19	3.76	8.33	0.30	-1.55
2014	5.85	1.63	27.75	3.08	8.47	-0.01	-0.72	5.26	1.72	32.75	2.39	7.69	-0.11	-0.97
2015	5.70	1.51	26.44	3.31	8.15	-0.06	-0.65	5.39	1.60	29.66	3.10	8.03	0.03	-0.85
2016	6.29	1.54	24.41	3.66	8.64	-0.25	-1.04	5.78	1.71	29.60	3.37	8.22	-0.21	-1.44
2017	6.10	1.68	27.47	4.09	9.84	0.84	0.63	6.14	1.75	28.56	4.06	9.93	0.80	0.32
2018	5.61	1.75	31.20	3.24	8.56	0.26	-1.01	5.36	1.90	35.37	3.08	8.44	0.52	-1.27
2019	5.91	1.75	29.57	3.02	9.03	0.20	-0.54	5.65	1.66	29.31	2.81	8.22	0.07	-0.82
2020	6.16	1.83	29.71	4.30	9.74	0.59	-0.85	5.85	1.65	28.18	4.28	9.15	0.75	-0.58
2021	6.24	1.50	23.95	3.78	9.05	0.14	-0.26	6.00	1.45	24.21	4.07	9.06	0.72	0.21
2022	5.90	1.64	27.78	3.96	8.40	0.22	-1.72	5.92	1.59	26.88	3.50	8.22	0.08	-1.56

TABLE VIII. DF PARAMETER AND P-VALUE BASED ON KS TEST FOR ANALYZING SR DATA

DF	Ardal			DF	Faridan		
	Parameters	**Statistic**	**Rank**		**Parameters**	**Statistic**	**Rank**
GEV	k=-0.18925 σ=1.5589 μ=5.2919	0.16969	1	GEV	k=-0.21368 σ=1.6772 μ=4.914	0.14995	1
G	α=14.136 β=0.42034	0.17318	2	G	α=11.259 β=0.49594	0.16301	2
W	α=3.8606 β=6.3056	0.17328	3	Na	m=3.1487 Ω=33.718	0.16604	3
IG	λ=83.995 μ=5.9419	0.17961	4	BS	α=0.2979 β=5.3465	0.16733	4
BS	α=0.26135 β=5.7456	0.17983	5	LN	σ=0.29609 μ=1.6772	0.16735	5
LN	σ=0.26018 μ=1.7487	0.18013	6	LL	α=4.7379 β=5.1435	0.16888	6
Na	m=3.8188 Ω=37.596	0.18483	7	IG	λ=62.87 μ=5.5839	0.16918	7
W-3P	α=0.82014 β=2.2016 γ=3.8836	0.18527	8	W	α=3.3814 β=5.9625	0.17315	8
N	σ=1.5804 μ=5.9419	0.19608	9	N	σ=1.6641 μ=5.5839	0.17425	9
LL	α=5.4193 β=5.5401	0.20239	10	L	σ=0.91748 μ=5.5839	0.19407	10
K	α_1=0.97025 α_2=1.0674 a=3.8836 b=8.6518	0.21235	11	W-3P	α=0.86229 β=1.9416 γ=3.3727	0.23268	11
L	σ=0.87131 μ=5.9419	0.21723	12	K	α_1=0.75667 α_2=1.5287 a=3.3727 b=8.6812	0.23604	12
R	σ=4.7409	0.28503	13	R	σ=4.4553	0.24914	13

Based on the findings in Table IX, the following can be concluded:

- In Faridan, the PV system produces the most electricity annually, reaching a peak of 10,932.52 kWh. The minimum annual electricity generation from the PV system is 10,283.56 kWh in Ardal. On average, the PV system generates around 10,608.04 kWh per year.

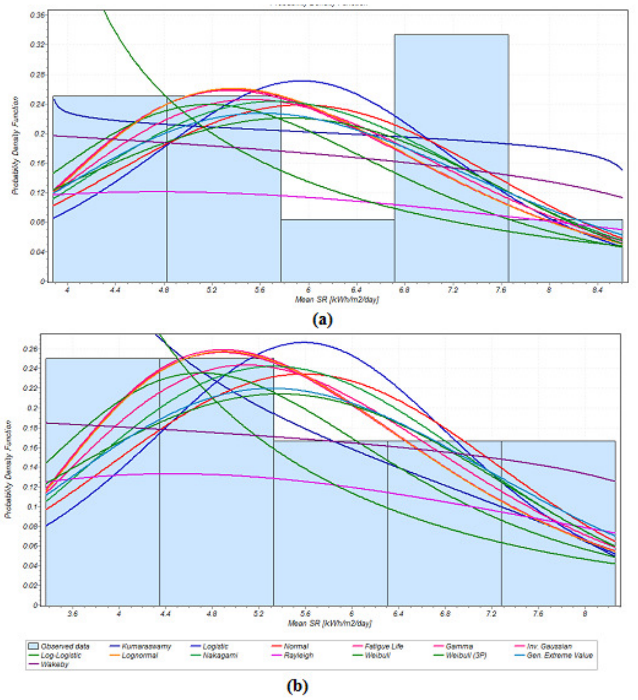

Fig. 4. PDF distributions comparison for analyzing SR data: (a) Ardal and (b) Faridan.

- Faridan also records the highest annual electricity generation from the wind system, with a maximum of 8,933.17 kWh. In Ardal, the wind system's annual generation is at its lowest, with a minimum of 6,724.77 kWh. On average, the wind system generates approximately 7,828.97 kWh annually.
- The efficiency of the PV system in Faridan reaches a maximum capacity factor of 24.96%, indicating effective utilization of the available sunlight. In Ardal, the PV system's capacity factor is at its lowest, with a minimum of 23.81%. On average, the PV system operates at a capacity factor of approximately 24.38%.
- Similarly, in Faridan, the wind system achieves a maximum capacity factor of 20.40%, showcasing its efficient conversion of available wind energy into electricity. In Ardal, the wind system's capacity factor is the lowest at 15.35%. On average, the wind system maintains a capacity factor of approximately 17.88%.
- The maximum simple payback period is 15.17 years in Ardal, the minimum is 12.99 years in Faridan, and the average is approximately 14.08 years. Similarly, the maximum equity payback period is 6.68 years in Ardal, the minimum is 5.41 years in Faridan, and the average is approximately 6.05 years.
- The maximum NPV is $9,377.86 in Faridan, the minimum is $5,945.58 in Ardal, and the average is approximately USD 7,161.72. A positive NPV not only demonstrates financial viability but also underscores the long-term sustainability of renewable energy projects by reducing energy costs and potentially generating revenue from excess energy production. Furthermore, the environmental benefits of reduced greenhouse gas emissions are implicit. Additionally, ALCS quantifies the annual financial savings generated by the project. In this context, the highest annual savings are USD 1,195.68/year in Faridan, while the lowest is USD 758.06/year in Ardal. The average ALCS is approximately USD 976.87/year.
- Energy Production Cost (EPC) signifies the cost of producing 1 kWh of electricity. It is found that the maximum cost is 0.1086 kWh/USD in Ardal and the minimum is 0.0930 kWh/USD in Faridan, whereas the average is approximately 0.1008 kWh/USD.
- Reducing GHG emissions promotes environmental sustainability by lowering the carbon footprint. It is found that the reduction is 11.48 tCO_2 in Faridan and 9.82 tCO_2 in Ardal, while the average is approximately 10.65 tCO_2

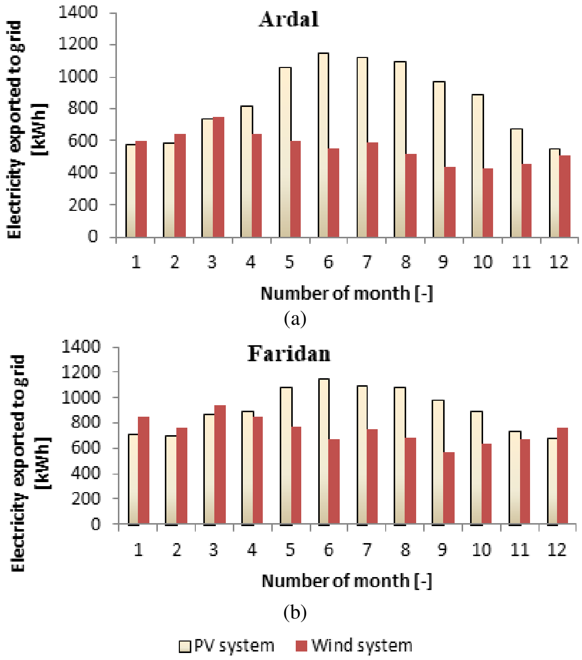

Fig. 5. Monthly variation of EGE of proposed systems.

TABLE IX. DF PARAMETERS AND P-VALUE BASED ON THE KS TEST FOR ANALYZING SR DATA

Parameters	Ardal	Faridan
Annual-PV system [kWh]	10283.56	10932.52
Annual wind system [kWh]	6724.77	8933.17
Capacity factor -PV system [%]	23.81	24.96
Capacity factor -wind system [%]	15.35	20.40
Gross annual GHG emission reduction [tCO2]	9.82	11.48
Simple payback [Year]	15.17	12.99
Equity payback [Year]	6.68	5.41
Net Present Value [USD]	5945.58	9377.86
Annual life cycle savings [USD/year]	758.06	1195.68
Energy production cost [kWh/USD]	0.1086	0.0930

Moreover, yearly cash flows in terms of cumulative and pre-tax values are crucial for assessing the financial viability and attractiveness of a project. They provide a comprehensive view of a project's financial performance over time, including its ability to generate returns on investment and its economic sustainability. These metrics aid decision-makers, investors, and project developers in evaluating projects and making informed financial and strategic choices. Cumulative cash flows represent the running total of cash inflows and outflows over time, usually on an annual basis. They accumulate year by year and provide insight into the project's overall financial performance throughout its lifespan. Cumulative cash flows help stakeholders understand the project's financial trajectory, including when it starts generating profits or returns on investment. They are crucial because they reveal the project's financial health over time and whether it is on track to recover its initial investment and generate a profit. Pre-tax cash flows refer to the cash inflows and outflows before accounting for income taxes. They are important because they reflect the project's financial performance in its purest form, without the influence of tax considerations. Analyzing pre-tax cash flows allows stakeholders to assess the project's economic viability and profitability based solely on its operational and financial characteristics. It helps in making investment decisions and evaluating the project's attractiveness to potential investors. Figure 6 provides an overview of the cash flow throughout the lifespan of wind farm and solar plant projects in the chosen region.

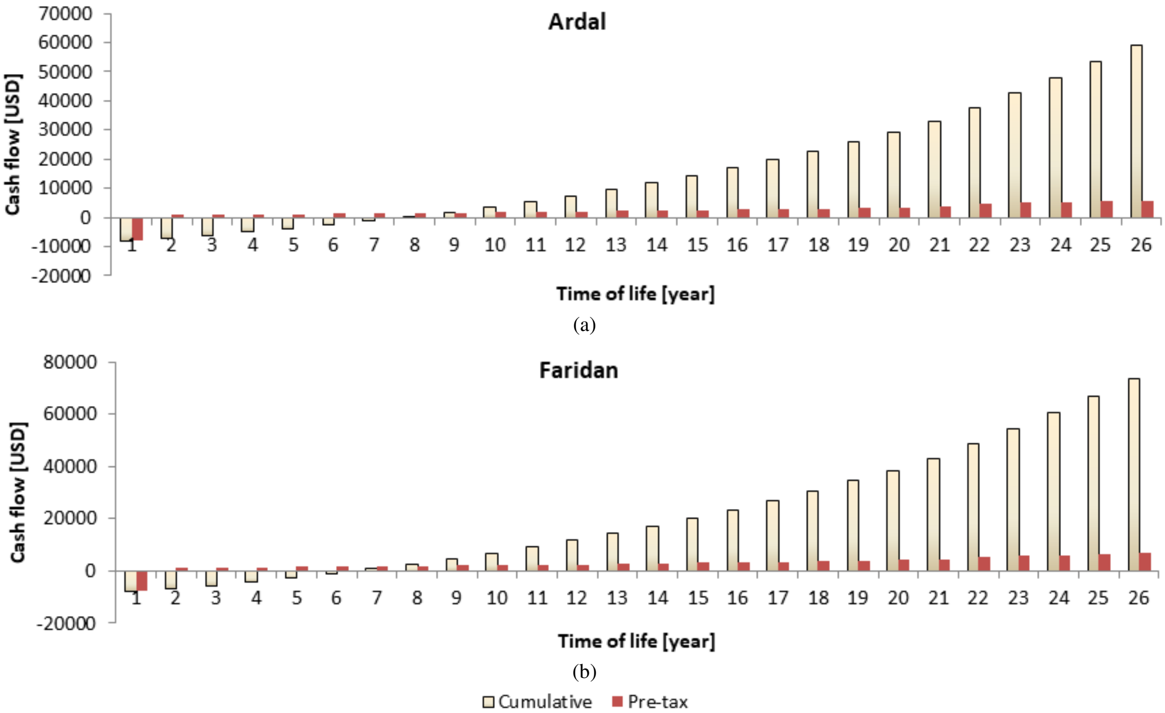

Fig. 6. Cumulative and pre-tax cash flow for all projects.

IV. DISCUSSION

The Sustainable Development Goals provide an inspiring framework for energy sector initiatives and policies, guiding them towards sustainability. Global energy demand is rising, leading to increased carbon emissions and environmental degradation. In response, Sustainable Development Goal 7 aims to provide "modern, reliable, and environmentally friendly energy for all" by 2030 [26]. Solar and wind energy undoubtedly support these endeavors and enhance technical and economic efforts to achieve the Sustainable Development Goals. An example of these ambitious projects is the installation of grid-connected vertical-axis hybrid wind turbines and PV tracking systems in high-altitude areas, representing a major step towards sustainable goals. High-altitude solar and wind energy are widely considered the most promising sources of renewable energy [27]. This paper represented the examination of high-altitude wind and solar energy potential in the regions of Ardal and Faridan, Iran for the first time utilizing the MERRA-2 dataset. To analyze the characteristics of wind and solar radiation data, 13 distribution functions were employed. According to the study's results, it was observed that the GEV DF displayed the lowest KS value. This shows that the GEV DF provides the best fit for the wind speed and solar radiation data, suggesting its suitability for modeling these datasets. Moreover, the obtained WPD values categorize the selected locations into power class 1, which signifies relatively low wind energy potential. Consequently, it is advisable to employ small-scale wind turbines in these areas to efficiently tap into the limited wind energy resources. On the other hand, both locations exhibit superb solar potential, suggesting that they are highly suitable for harnessing solar energy resources. Furthermore, this paper presented a technical and economic feasibility study of a VAWT and PV tracking system for electricity production.

Based on the findings of this study, it has been determined that the total energy production from the hybrid system is 17,008.33 kWh for Ardal and 19,865.69 kWh for Faridan. Moreover, the PV system competence varies between the two regions, with Faridan achieving a maximum capacity factor of 24.96%, denoting effective utilization of available sunlight, while Ardal achieved 23.81%, with an average of approximately 24.38%. Similarly, in Faridan, the wind system demonstrates efficiency with a maximum capacity factor of 20.40%, successfully converting wind resources into electricity. In contrast, Ardal's wind system has the lowest capacity factor at 15.35%, with an approximate average of 17.88%. These results are supported by several previous studies. As mentioned in [28], the economic viability of a project is measured by considering its NPV and payback period. In the case of this project, the NPV, which represents the disparity between the present value of cash inflows and cash outflows over a specific time frame for all locations, yielded positive results. This positive NPV signifies that the project is financially and economically viable [29-32]. Besides, it is observed that simple and equity payback period is within the range of 12.99-15.17 years and 5.41-6.68 years, respectively. These results are in accordance with the findings of several previous studies. For example, authors in [31] reported CF values ranging from 31.1% to 49% for 50 m hub-height turbines and 37.3% to 56.6% for 75m hub-height turbines. Authors in [33] observed varying values for simple payback and CF in the range of 1.9 to 27.3 years and 4.5% to 37.2%, respectively, for a BWT 61 m–800 kW wind turbine. In [34], it was found that the payback period for various 100 MW wind farms ranged from 6.34 to 19.9 years. Authors in [35] noted that CF values for various wind turbines fell between 32% and 38%. Authors in [36] reported CF values spanning from 6.8% to 47.6% for different wind turbines with varying characteristics. Authors in [32] proposed a PV system had an annual CF ranging from 20.70% to 21.70%. Authors in [32] found that the payback period for their developed PV system ranged from 13.6 to 14.6 years. Authors in [37] reported annual CF values ranging from 17.5% to 20.03% and simple payback period values within the range of 6.38 years to 7.00 years. Authors in [38] outlined a CF value of 22 for 12.25 kW grid-connected PV systems.

Moreover, this study's findings reveal that the highest energy production cost is 0.1086 kWh/USD in Ardal, while the lowest is 0.0930 kWh/USD in Faridan, with an average of approximately 0.1008 kWh/USD. These outcomes are corroborated by several scientific investigations. For example, authors in [33] observed that the LCOE for a 61 m–800 kW BWT wind turbine falls in the range of 0.04-0.43 USD. Authors in [35] noted LCOE values ranged from 0.255 USD/kWh to 0.306 USD/kWh. Authors in [36] reported CF values spanning from 6.8% to 47.6% for different wind turbines with diverse characteristics. Authors in [5] described LCOE values varying from 0.08703 USD/kWh to 0.01025 USD/kWh for a 5 kW Vertical Axis Wind Generator-V and LCOE values ranging from 0.036 USD/kWh to 0.049 USD/kWh for a 5 kW grid-connected PV system. Authors in [32] reported LCOE values for their proposed PV system varying from 0.128 USD/kWh to 0.135 USD/kWh. Authors in [38] estimated an LCOE value of 0.0382 USD/kWh for a developed PV system.

According to the Iran Energy Report 2022, electricity cost has shown an annual rise of approximately 20% since 2019, reaching 0.0024 USD/kWh for households and 0.0034 USD/kWh for industrial consumers in 2021. It is found that the energy production cost from the proposed system is higher than the electricity tariff. However, there are still several benefits from the developed systems such as (1) reduced reliance on external power sources, especially in remote areas or during power outages, (2) reduced greenhouse gas emissions and carbon footprint, (3) provision of a stable electricity source and reduced vulnerability to energy price fluctuations, (4) earning income through net metering or feed-in tariffs, and (5) leading to more stable and efficient energy infrastructure.

Additionally, the gross annual greenhouse gas emission reduction quantifies the decrease in greenhouse gas emissions attributable to the renewable energy project. These emissions are significant contributors to global warming and climate change. The study reported 11.48 tCO_2 reduction in Faridan, and 9.82 tCO_2 in Ardal, with an average of around 10.65 tCO_2. By mitigating these tons of CO_2 equivalent, the project contributes to the realization of Sustainable Development Goal 15 (SDG 15): Life on Land.

V. CONCLUSIONS AND FUTUER WORK

The case study in this research demonstrates the possible technical and economic feasibility and develops a system to meet household energy needs. This research can serve as a framework to evaluate the practicability of the prospective small-scale hybrid wind system in Iran and other developing countries. In future studies, a hardware implementation of the system suggested may be carried out with detailed performance analysis, paving the way for its eventual dissemination and widespread adoption.

Exploring the achievability of wind and solar power in high-altitude areas is essential to maximizing renewable energy sources. These regions offer unique advantages, including stronger, more consistent wind patterns and greater exposure to sunlight. Harnessing these resources not only enhances clean energy production but also carries environmental benefits. It reduces greenhouse gas emissions, combats climate change, and has the potential to improve air quality. Furthermore, this transformation creates opportunities for sustainable development and job creation, thus benefiting local communities socially and economically. Such systems also hold the promise of improved public health, thanks to reduced pollution and cleaner air. Hence, prioritizing the environmental impact assessment of small-scale hybrid systems (wind and solar) to enhance the social acceptance of renewable energy technologies should be the main focus of future research. Besides, a comprehensive risk analysis of small-scale hybrid systems, incorporating wind and solar energy sources, is essential to assess the financial viability of such projects in the future. This analysis should entail various factors, including political, regulatory, and market risks, which can significantly impact these initiatives success. A thorough risk analysis should consider these factors, employ risk mitigation strategies, and develop contingency plans to ensure the financial viability of small-scale hybrid systems. This will help project developers, investors, and policymakers make informed decisions and increase the likelihood of renewable energy projects to be successful.

REFERENCES

[1] K. Obaideen *et al.*, "On the contribution of solar energy to sustainable developments goals: Case study on Mohammed bin Rashid Al Maktoum Solar Park," *International Journal of Thermofluids*, vol. 12, Nov. 2021, Art. no. 100123, https://doi.org/10.1016/j.ijft.2021.100123.

[2] T. Hak, S. Janouskova, and B. Moldan, "Sustainable Development Goals: A need for relevant indicators," *Ecological Indicators*, vol. 60, pp. 565–573, Jan. 2016, https://doi.org/10.1016/j.ecolind.2015.08.003.

[3] C. R. Kumar. J and M. A. Majid, "Renewable energy for sustainable development in India: current status, future prospects, challenges, employment, and investment opportunities," *Energy, Sustainability and Society*, vol. 10, no. 1, Dec. 2020, Art. no. 2, https://doi.org/10.1186/s13705-019-0232-1.

[4] L. S. Paraschiv and S. Paraschiv, "Contribution of renewable energy (hydro, wind, solar and biomass) to decarbonization and transformation of the electricity generation sector for sustainable development," *Energy Reports*, vol. 9, pp. 535–544, Sep. 2023, https://doi.org/10.1016/j.egyr.2023.07.024.

[5] Y. Kassem and M. H. A. Abdalla, "Modeling predictive suitability to identify the potential of wind and solar energy as a driver of sustainable development in the Red Sea state, Sudan," *Environmental Science and Pollution Research*, vol. 29, no. 29, pp. 44233–44254, Jun. 2022, https://doi.org/10.1007/s11356-022-19062-9.

[6] Y. Kassem, H. Camur, and O. a. M. Abughinda, "Solar Energy Potential and Feasibility Study of a 10MW Grid-connected Solar Plant in Libya," *Engineering, Technology & Applied Science Research*, vol. 10, no. 4, pp. 5358–5366, Aug. 2020, https://doi.org/10.48084/etasr.3607.

[7] Y. Kassem, H. Camur, and A. A. S. Mosbah, "Feasibility Analysis of the Wind Energy Potential in Libya using the RETScreen Expert," *Engineering, Technology & Applied Science Research*, vol. 13, no. 4, pp. 11277–11289, Aug. 2023, https://doi.org/10.48084/etasr.6007.

[8] S. Solaymani, "A Review on Energy and Renewable Energy Policies in Iran," *Sustainability*, vol. 13, no. 13, Jan. 2021, Art. no. 7328, https://doi.org/10.3390/su13137328.

[9] H. Gökçekuş and Y. Kassem, Eds., *Climate Change, Natural Resources and Sustainable Environmental Management*, 1st ed. Springer, 2022.

[10] Y. Kassem, H. Camur, and R. A. F. Aateg, "Exploring Solar and Wind Energy as a Power Generation Source for Solving the Electricity Crisis in Libya," *Energies*, vol. 13, no. 14, Jan. 2020, Art. no. 3708, https://doi.org/10.3390/en13143708.

[11] M. Tsangas, A. A. Zorpas, and M. Jeguirim, "Sustainable renewable energy policies and regulations, recent advances, and challenges," in *Renewable Energy Production and Distribution*, vol. 1, M. Jeguirim, Ed. New York, NY, USA: Academic Press, 2022, pp. 449–465.

[12] D. Nugent and B. K. Sovacool, "Assessing the lifecycle greenhouse gas emissions from solar PV and wind energy: A critical meta-survey," *Energy Policy*, vol. 65, pp. 229–244, Feb. 2014, https://doi.org/10.1016/j.enpol.2013.10.048.

[13] H. S. A. Lagili, A. Kiraz, Y. Kassem, and H. Gokcekus, "Wind and Solar Energy for Sustainable Energy Production for Family Farms in Coastal Agricultural Regions of Libya Using Measured and Multiple Satellite Datasets," *Energies*, vol. 16, no. 18, Jan. 2023, Art. no. 6725, https://doi.org/10.3390/en16186725.

[14] L. Qiu, L. He, H. Lu, and D. Liang, "Systematic potential analysis on renewable energy centralized co-development at high altitude: A case study in Qinghai-Tibet plateau," *Energy Conversion and Management*, vol. 267, Sep. 2022, Art. no. 115879, https://doi.org/10.1016/j.enconman.2022.115879.

[15] S. Zhou *et al.*, "A novel multi-objective scheduling model for grid-connected hydro-wind-PV-battery complementary system under extreme weather: A case study of Sichuan, China," *Renewable Energy*, vol. 212, pp. 818–833, Aug. 2023, https://doi.org/10.1016/j.renene.2023.05.092.

[16] R. Gelaro *et al.*, "The Modern-Era Retrospective Analysis for Research and Applications, Version 2 (MERRA-2)," *Journal of Climate*, vol. 30, no. 14, pp. 5419–5454, Jul. 2017, https://doi.org/10.1175/jcli-d-16-0758.1.

[17] Y. Kassem, H. Gokcekus, and W. Janbein, "Predictive model and assessment of the potential for wind and solar power in Rayak region, Lebanon," *Modeling Earth Systems and Environment*, vol. 7, no. 3, pp. 1475–1502, Sep. 2021, https://doi.org/10.1007/s40808-020-00866-y.

[18] Y. Kassem, H. Camur, M. T. Adamu, T. Chikowero, and T. Apreala, "Prediction of Solar Irradiation in Africa using Linear-Nonlinear Hybrid Models," *Engineering, Technology & Applied Science Research*, vol. 13, no. 4, pp. 11472–11483, Aug. 2023, https://doi.org/10.48084/etasr.6131.

[19] Y. Kassem, H. Camur, and S. M. A. Alhuoti, "Solar Energy Technology for Northern Cyprus: Assessment, Statistical Analysis, and Feasibility Study," *Energies*, vol. 13, no. 4, Jan. 2020, Art. no. 940, https://doi.org/10.3390/en13040940.

[20] Y. Kassem, H. Gokcekus, and A. Guvensoy, "Techno-Economic Feasibility of Grid-Connected Solar PV System at Near East University Hospital, Northern Cyprus," *Energies*, vol. 14, no. 22, Jan. 2021, Art. no. 7627, https://doi.org/10.3390/en14227627.

[21] L. He, A. Lin, X. Chen, H. Zhou, Z. Zhou, and P. He, "Assessment of MERRA-2 Surface PM2.5 over the Yangtze River Basin: Ground-based Verification, Spatiotemporal Distribution and Meteorological Dependence," *Remote Sensing*, vol. 11, no. 4, Jan. 2019, Art. no. 460, https://doi.org/10.3390/rs11040460.

[22] L. Qi, P. Zheng, X. Wu, W. Duan, L. Li, and Z. Zhang, "A hybrid wind-photovoltaic power generation system based on the foldable umbrella mechanism for applications on highways," *Solar Energy*, vol. 208, pp. 368–378, Sep. 2020, https://doi.org/10.1016/j.solener.2020.07.082.

[23] S. A. Ginanjar, B. Halimi, and A. Rizqiawan, "Solar PV-Wind Turbine Integration in Hydrogen Production to Generate Electricity through Fuel Cell," in *3rd International Conference on High Voltage Engineering and Power Systems*, Bandung, Indonesia, Oct. 2021, pp. 211–216, https://doi.org/10.1109/ICHVEPS53178.2021.9600965.

[24] Y. Kassem, H. Gokcekus, and A. M. S. Essayah, "Wind Power Potential Assessment at Different Locations in Lebanon: Best–Fit Probability Distribution Model and Techno-Economic Feasibility," *Engineering, Technology & Applied Science Research*, vol. 13, no. 2, pp. 10578–10587, Apr. 2023, https://doi.org/10.48084/etasr.5686.

[25] M. M. Alayat, Y. Kassem, and H. Çamur, "Assessment of Wind Energy Potential as a Power Generation Source: A Case Study of Eight Selected Locations in Northern Cyprus," *Energies*, vol. 11, no. 10, Oct. 2018, Art. no. 2697, https://doi.org/10.3390/en11102697.

[26] A. Sanchez, Q. Zhang, M. Martin, and P. Vega, "Towards a new renewable power system using energy storage: An economic and social analysis," *Energy Conversion and Management*, vol. 252, Jan. 2022, Art. no. 115056, https://doi.org/10.1016/j.enconman.2021.115056.

[27] M. Ban, L. Perkovic, N. Duic, and R. Penedo, "Estimating the spatial distribution of high altitude wind energy potential in Southeast Europe," *Energy*, vol. 57, pp. 24–29, Aug. 2013, https://doi.org/10.1016/j.energy.2012.12.045.

[28] T. S. Ong and C. H. Thum, "Net Present Value and Payback Period for Building Integrated Photovoltaic Projects in Malaysia," *International Journal of Academic Research in Business and Social Sciences*, vol. 3, no. 2, pp. 153–171, 2013.

[29] Y. Kassem, H. Gokcekus, and R. Gokcekus, "Economic Feasibility of Large-Scale Renewable Energy Projects in Mountain Location, Northern Cyprus," in *5th International Conference on Natural Resources and Sustainable Environmental Management*, Nicosia, Cyprus, Nov. 2021, pp. 66–71, https://doi.org/10.1007/978-3-031-04375-8_8.

[30] H. Camur, Y. Kassem, and E. Alessi, "A Techno-Economic Comparative Study of a Grid-Connected Residential Rooftop PV Panel: The Case Study of Nahr El-Bared, Lebanon," *Engineering, Technology & Applied Science Research*, vol. 11, no. 2, pp. 6956–6964, Apr. 2021, https://doi.org/10.48084/etasr.4078.

[31] A. Allouhi *et al.*, "Evaluation of wind energy potential in Morocco's coastal regions," *Renewable and Sustainable Energy Reviews*, vol. 72, pp. 311–324, May 2017, https://doi.org/10.1016/j.rser.2017.01.047.

[32] A. B. Owolabi, B. E. K. Nsafon, J. W. Roh, D. Suh, and J.-S. Huh, "Validating the techno-economic and environmental sustainability of solar PV technology in Nigeria using RETScreen Experts to assess its viability," *Sustainable Energy Technologies and Assessments*, vol. 36, Dec. 2019, Art. no. 100542, https://doi.org/10.1016/j.seta.2019.100542.

[33] K. A. Adeyeye, N. Ijumba, and J. S. Colton, "A Techno-Economic Model for Wind Energy Costs Analysis for Low Wind Speed Areas," *Processes*, vol. 9, no. 8, Aug. 2021, Art. no. 1463, https://doi.org/ 10.3390/pr9081463.

[34] M. A. Alsaad, "Wind energy potential in selected areas in Jordan," *Energy Conversion and Management*, vol. 65, pp. 704–708, Jan. 2013, https://doi.org/10.1016/j.enconman.2011.12.037.

[35] A. Ucar and F. Balo, "Investigation of wind characteristics and assessment of wind-generation potentiality in Uludağ-Bursa, Turkey," *Applied Energy*, vol. 86, no. 3, pp. 333–339, Mar. 2009, https://doi.org/10.1016/j.apenergy.2008.05.001.

[36] H. D. Ammari, S. S. Al-Rwashdeh, and M. I. Al-Najideen, "Evaluation of wind energy potential and electricity generation at five locations in Jordan," *Sustainable Cities and Society*, vol. 15, pp. 135–143, Jul. 2015, https://doi.org/10.1016/j.scs.2014.11.005.

[37] K. Mohammadi, M. Naderi, and M. Saghafifar, "Economic feasibility of developing grid-connected photovoltaic plants in the southern coast of Iran," *Energy*, vol. 156, pp. 17–31, Aug. 2018, https://doi.org/ 10.1016/j.energy.2018.05.065.

[38] A. A. Imam, Y. A. Al-Turki, and S. K. R., "Techno-Economic Feasibility Assessment of Grid-Connected PV Systems for Residential Buildings in Saudi Arabia—A Case Study," *Sustainability*, vol. 12, no. 1, Jan. 2020, Art. no. 262, https://doi.org/10.3390/su12010262.